

## The NMR Spectra of Triethylsilane and Triethylhalogenosilane

By Osamu YAMAMOTO and Kikuko HAYAMIZU

(Received July 17, 1964)

The proton magnetic resonance spectra of a number of metal ethyl compounds have been studied, and attempts have been made to correlate the internal chemical shift,  $\delta$ , between the methyl and the methylene protons in the ethyl group ( $\nu_{\text{CH}_3} - \nu_{\text{CH}_2}$ ) with the electronegativity,  $x$ , of the metal attached to the ethyl group. Although the empirical relationship between  $\delta$  and  $x$  proposed by Dailey and Shoolery<sup>1)</sup> approximately holds over a wide variety of metals, considerable deviations are observed when one of the ethyl group in the metal compounds is replaced by a halogen atom.<sup>2,3)</sup> This is due to the magnetic anisotropy of the halogen atom or the C-X bond, where X denotes a halogen atom. Since the order of magnitude of the magnetic anisotropy effect of halogens in aliphatic compounds has been observed to increase with an increase in their atomic weight,<sup>4)</sup> the deviation of the  $\delta$  value

from the simple Dailey and Shoolery relationship will increase in the order of fluorine, chlorine, bromine and iodine. Hence, when a more electronegative halogen atom substitutes on the metal, the  $\delta$  value decreases in a manner contrary to that expected from the simple inductive mechanism. This trend has been observed in diethylaluminum monohalides.<sup>3)</sup>

In connection with this, the NMR spectra of triethylsilane and triethylhalogenosilane were studied in the present work, and accurate  $\delta$  and  $J$  (coupling constant) values were given through a rigorous analysis of the spectra. Although triethylchloro- and triethylbromosilane show the  $A_3B_2$  spectra for their ethyl groups, which can be analyzed in the manner described in the previous paper,<sup>3)</sup> triethylsilane and triethylfluorosilane give the  $A_3B_2X$  spectra. The analysis of the  $A_3B_2X$  system has been already made by Narasimhan and Rogers<sup>5)</sup> using the model of the composite spin particles which have total spin angular momenta of 3/2, 1, and 1/2 respectively. In the present work this method is also followed, though the spin-spin coupling between A and X is also taken

1) B. P. Dailey and J. N. Shoolery, *J. Am. Chem. Soc.*, **77**, 3977 (1955).

2) P. T. Narasimhan and M. T. Rogers, *ibid.*, **82**, 5983 (1960).

3) O. Yamamoto, *This Bulletin*, **36**, 1463 (1963).

4) L. M. Jackman, "Applications of Nuclear Magnetic Resonance Spectroscopy in Organic Chemistry," Pergamon Press, New York (1959), p. 53.

5) P. T. Narasimhan and M. T. Rogers, *J. Chem. Phys.*, **33**, 727 (1960).

into account. (This corresponds to the coupling between the methyl protons and fluorine or hydrogen directly attached to silicon.) While such a long-range coupling can be, practically speaking, extremely small in most organic compounds, it may not be negligible when such an atom as fluorine is present in the coupling system.<sup>6)</sup>

Hereafter, in the notations  $A_3B_2$  and  $A_3B_2X$ , A and B refer to methyl and methylene protons in an ethyl group respectively, and X to hydrogen or fluorine directly attached to silicon. Thus, for example,  $J_{AB}$  means the coupling constant between the methyl and the methylene protons in the ethyl group.

### Experimental

Triethylsilane was prepared from trichlorosilane and ethylmagnesium bromide;<sup>7)</sup> triethylfluorosilane and triethylchlorosilane were prepared by adding the corresponding ammonium halide to hexaethyldisiloxane in concentrated sulfuric acid<sup>8)</sup> triethylbromosilane was prepared by dropping liquid bromine into phenyltriethylsilane.<sup>9)</sup> The purity of the samples was examined by means of their infrared absorption spectra and by gas chromatography.

The NMR spectra of the compounds were obtained by means of a Varian Associates DP-60 spectrometer at 60, 40, and 15 Mc./sec., together with a Varian HR-100 spectrometer at 100 Mc./sec. for the pure liquid samples degassed in a high-vacuum apparatus.

### Results and Discussion

The spectra for all of the compounds obtained at 60 Mc./sec. are illustrated in Fig. 1—4, together with the calculated spectral lines (shown at the bottoms of the figures). In addition, the spectra at 40 and at 100 Mc./sec. were also obtained for triethylsilane and triethylfluorosilane, which show the more complex spectra due to the  $A_3B_2X$  spin system than do the other two, with the  $A_3B_2$  pattern.

The analyses of the spectra as an  $A_3B_2$  or  $A_3B_2X$  system were accomplished with a NEAC-2101 digital computer. The procedure was the same for the  $A_3B_2$  system as that described in the previous paper.<sup>3)</sup> For the analysis of the  $A_3B_2X$  system, the calculations were repeated until a good agreement in the coupling constants and the chemical shift values was obtained among 40, 60, and 100 Mc./sec. spectra by using the least-squares method.

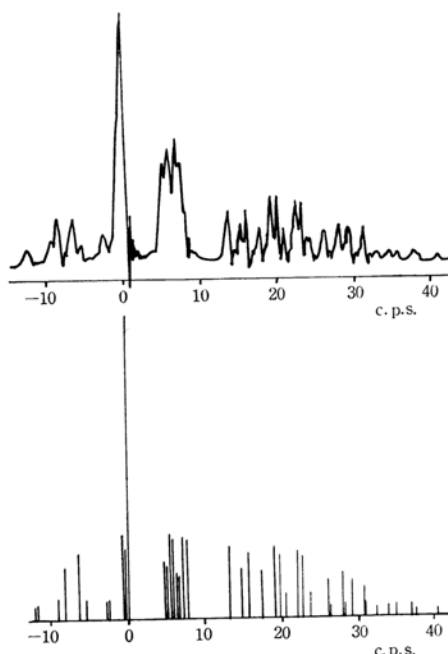


Fig. 1. The observed and the calculated spectra of  $\text{SiH}(\text{C}_2\text{H}_5)_3$  at 60 Mc./sec.

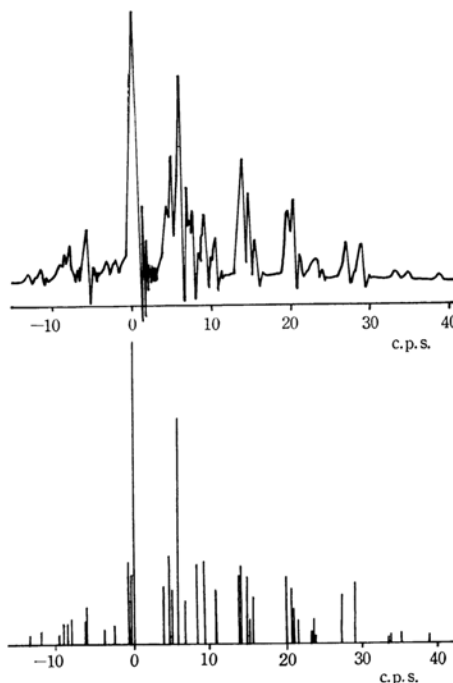


Fig. 2. The observed and the calculated spectra of  $\text{SiF}(\text{C}_2\text{H}_5)_3$  at 60 Mc./sec.

The coupling constants and chemical shift values thus obtained are shown in Table I. The numerical details of the calculations for triethylsilane and triethylfluorosilane at 60

6) D. D. Elleman, L. C. Brown, and D. Williams, *J. Mol. Spectry.*, **7**, 322 (1961).

7) F. C. Whitmore, E. W. Pietrusza and L. H. Sommer, *J. Am. Chem. Soc.*, **69**, 2108 (1947).

8) P. A. Di Giorgio, W. A. Strong, L. H. Sommer and F. C. Whitmore, *ibid.*, **68**, 1380 (1946).

9) B. O. Pray, L. H. Sommer, G. M. Goldberg, G. T. Kerr, P. A. Di Giorgio and F. W. Whitmore, *ibid.*, **70**, 433 (1948).

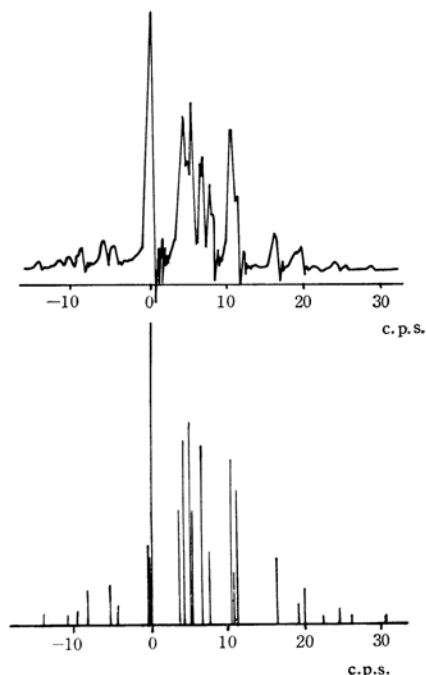


Fig. 3. The observed and the calculated spectra of  $\text{SiCl}(\text{C}_2\text{H}_5)_3$  at 60 Mc./sec.

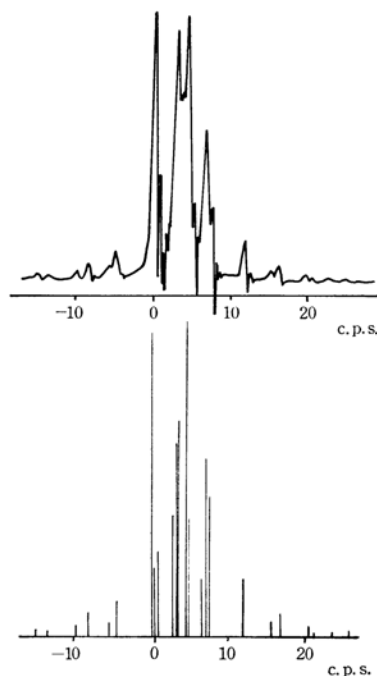


Fig. 4. The observed and the calculated spectra of  $\text{SiBr}(\text{C}_2\text{H}_5)_3$  at 60 Mc./sec.

Mc./sec. are given in Tables II and III respectively. Similar good agreements between the observed and the calculated spectra were also obtained at other resonant frequencies.

The coupling constants,  $J_{\text{BX}}$ , can also be obtained from the X part of the  $\text{A}_3\text{B}_2\text{X}$  spectra. As is shown in Table I, the observed values are in agreement with the values obtained from the  $\text{A}_3\text{B}_2$  part of the spectra within the range of experimental error.

#### Coupling Constants in Triethylfluorosilane.—

In triethylsilane the long-range coupling constant,  $J_{\text{AX}}$ , is practically zero, as is usually observed for two protons which are more than three bonds removed from each other in aliphatic compounds. In triethylfluorosilane, however,  $J_{\text{AX}}$  definitely has a non-zero value,

as may be seen from Table I. In fact, the calculations taking no account of  $J_{\text{AX}}$  were tried at first, but in this case no overall agreement of the calculated coupling constants and chemical shift values was obtained among the spectra different in resonant frequencies.

The long-range coupling between protons and fluorines which are separated through four bonds from each other has been reported for fluorocarbon derivatives.<sup>6)</sup> The order of magnitude of such coupling constants is from about 0.4 to 1.5 c.p.s., which is comparable with the value obtained,  $J_{\text{AX}}$ , for triethylfluorosilane. Further evidence for the long-range coupling is obtained from the 15 Mc./sec. spectrum of this compound. The most intense central line in the  $\text{A}_3\text{B}_2$  spectrum splits into two lines of equal

TABLE I. CHEMICAL SHIFTS AND COUPLING CONSTANTS OF TRIETHYLSILANE AND TRIETHYLHALOGENOSILANE

	$\text{SiH}(\text{C}_2\text{H}_5)_3$	$\text{SiF}(\text{C}_2\text{H}_5)_3$	$\text{SiCl}(\text{C}_2\text{H}_5)_3$	$\text{SiBr}(\text{C}_2\text{H}_5)_3$
$\delta_{\text{AB}}^*$ (p. p. m.)	0.40	0.32	0.22	0.16
$J_{\text{AB}}$ (c. p. s.)	7.9 <sub>2</sub>	8.0 <sub>5</sub>	7.9 <sub>8</sub>	7.7 <sub>7</sub>
$J_{\text{BX}}$ (c. p. s.)	3.0 <sub>6</sub>	5.8 <sub>6</sub>		
$J_{\text{AX}}$ (c. p. s.)	0.0 <sub>7</sub>	0.3 <sub>9</sub>		

Observed values from the X part of the spectrum

$\delta_{\text{AX}}$ (p. p. m.)	-2.70*	116.8**
$J_{\text{BX}}$ (c. p. s.)	3.0	5.7

\* Referred to the methyl signal. Thus these values have opposite signs to the internal chemical shifts  $\delta$ .

\*\*  $^{19}\text{F}$  resonance from  $\text{CFCl}_3$ .

TABLE II. OBSERVED AND CALCULATED SPECTRA OF TRIETHYLSILANE AT 60 Mc./sec.

Transition No.	Frequency c. p. s.		Relative intensity	
	Calcd.	Obs.	Calcd.	Obs.
CH <sub>3</sub> -transition				
1	-12.1	-11.9	1.1	2.2
2	-11.6		1.2	
3	-9.1	-9.0	1.0	4.9
4	-8.9		1.1	
5	-8.2	-8.1	2.0	
6	-8.2		2.2	
7	-6.4	-6.3	1.3	4.5
8	-6.4		2.0	
9	-6.3	-5.4	1.9	2.7
10	-5.3		1.6	
11	-2.7	-2.4	1.4	36.2
12	-2.4		1.5	
13	-0.8	0.0	3.4	35.8
14	-0.7		3.3	
15	-0.4	5.1	2.8	12.5
16	-0.3		2.8	
17	-0.0	5.9	12.0	12.4
18	0.0		12.0	
19	4.7	5.9	4.4	4.4
20	5.1		4.2	
21	5.5	6.8	6.6	4.8
22	5.9		6.3	
23	6.3	7.4	3.6	3.2
24	6.6		3.4	
25	6.9	7.4	6.6	3.6
26	7.3		6.1	

CH<sub>2</sub>-transition

1	13.0	12.9	5.7	4.7
2	14.8	14.6	4.0	7.7
3	15.6	15.6	5.1	3.6
4	17.4	17.5	3.7	12.5
5	18.9	18.9	5.7	12.4
6	19.7	19.6	5.1	4.4
7	20.5	20.4	2.0	4.8
8	21.9	21.8	5.3	1.2
9	22.6	22.7	4.9	3.2
10	23.6	23.6	2.0	3.6
11	26.0	26.0	3.0	1.2
12	26.3	26.8	1.0	1.0
13	28.0		1.2	2.2
14	28.0	28.0	2.4	0.7
15	28.2		1.2	0.8
16	29.1	29.1	3.0	
17	30.9	30.8	2.5	
18	31.0		1.2	
19	32.5	32.5	0.8	
20	33.9	33.7	0.9	
21	34.9	34.8	0.9	
22	37.0	37.1	0.9	
23	37.5		0.7	
24	40.3	40.2	0.7	

TABLE III. OBSERVED AND CALCULATED SPECTRA OF TRIETHYLFLUOROSILANE AT 60 Mc./sec.

Transition No.	Frequency c. p. s.		Relative intensity	
	Calcd.	Obs.	Calcd.	Obs.
CH <sub>3</sub> -transition				
1	-13.4	-13.1	0.8	0.5
2	-12.0	-11.7	1.1	1.1
3	-9.6	-9.5	0.8	5.2
4	-9.0		1.0	
5	-8.9	-8.8	0.8	4.8
6	-8.5		1.7	
7	8.1	-8.0	2.1	1.8
8	-6.2	-5.9	1.4	
9	-6.1		1.7	2.0
10	-6.1	-3.3	1.9	
11	-3.7		1.2	36.1
12	-2.5	-2.7	1.4	
13	-0.5	0.0	3.3	45.0
14	-0.4		3.2	
15	-0.3	6.3	2.7	1.2
16	-0.2		12.0	
17	-0.1	7.0	2.8	0.8
18	0.2		12.0	
19	4.0	4.3	4.6	0.7
20	4.7	5.2	7.1	
21	5.1	6.3	4.3	1.2
22	5.8		4.1	
23	5.9	7.6	6.5	0.8
24	5.9		7.5	
25	6.7	7.0	3.5	0.7
26	7.3	7.6	6.5	

CH<sub>2</sub>-transition

1	9.2	9.2	6.6	7.0
2	10.7	10.7	4.3	4.8
3	13.8	14.0	5.4	20.0
4	14.1		6.2	
5	15.0	14.9	5.3	12.9
6	15.2		2.1	
7	15.5	15.7	3.8	3.6
8	19.9	20.1	5.4	
9	20.5	20.9	4.9	3.2
10	21.0	20.9	2.9	
11	21.4	21.6	1.9	4.0
12	23.3	23.5	1.1	
13	23.6		2.0	1.2
14	24.0	27.4	0.6	
15	27.0		2.9	0.8
16	27.1	29.1	1.0	
17	28.9		1.1	0.7
18	29.0	33.6	2.3	
19	29.1		0.8	0.8
20	29.1	38.9	0.6	
21	33.4		0.5	0.7
22	33.5		0.7	
23	35.0	35.2	0.8	0.7
24	38.7	38.9	0.6	

intensity in the A<sub>3</sub>B<sub>2</sub>X system due to the coupling between the A and X spins, the separation between the two lines being just equal to  $J_{AX}$  (see Appendix). However, if  $J_{AX}$  is too small to be resolved under the conditions of a given magnetic field, the splitting is not observed. This is the case for the resonant frequency of 40 Mc./sec. or higher. The inhomogeneity,  $\Delta H$ , of the field may be

reduced by decreasing the static field,  $H_0$ , in such a manner that  $\Delta H/H_0 \sim \text{constant}$ .<sup>10)</sup> Thus, at the low static field, it may be possible to observe the splitting of two lines which can not be resolved in the higher field. As Fig. 5 shows, the two split lines are clearly realized at 15 Mc./sec., the separation of them being

10) A. Abragam, "The Principles of Nuclear Magnetism," Oxford University Press, London (1961), p. 64.

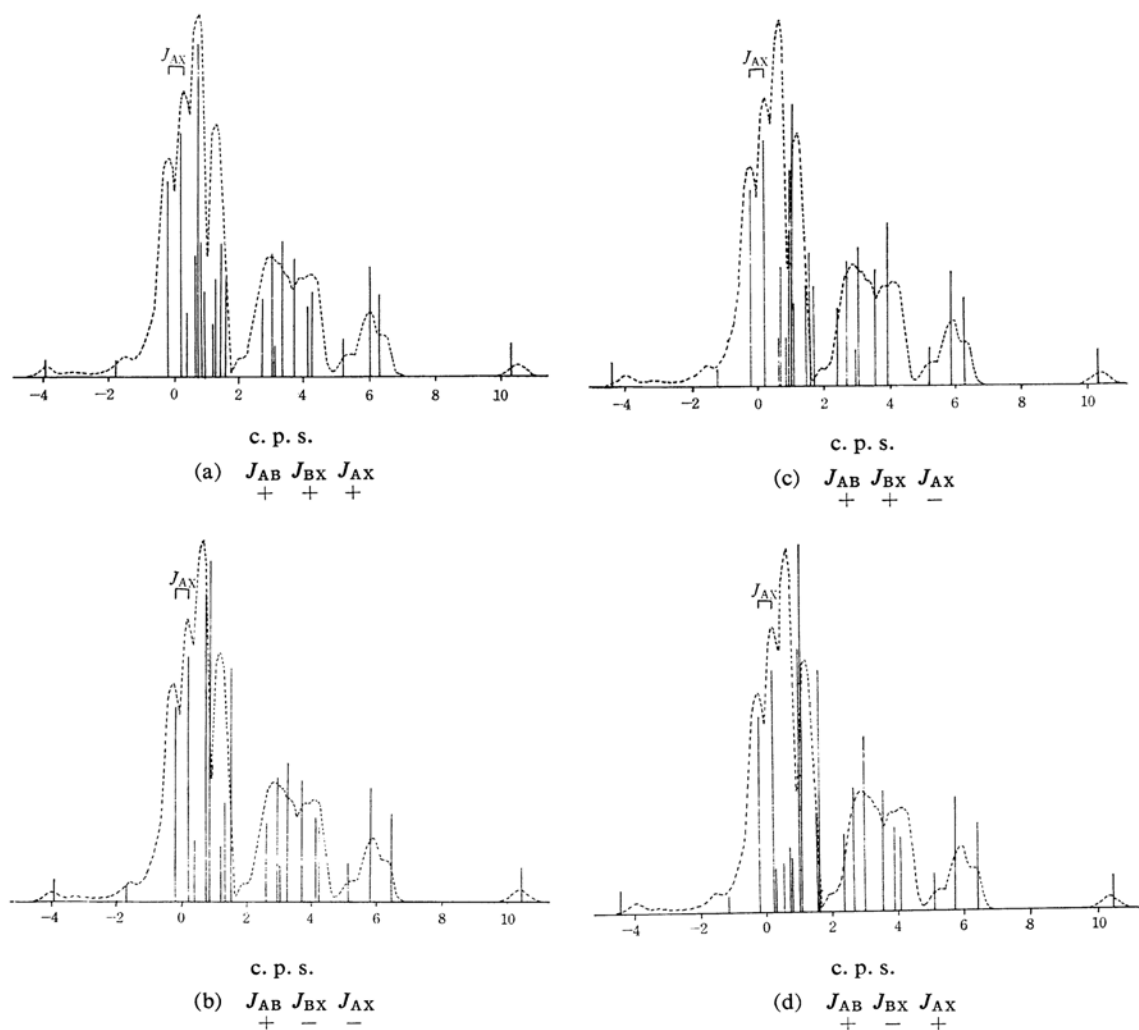


Fig. 5. The calculated spectra of  $\text{SiF}(\text{C}_2\text{H}_5)_3$  at 15.085 Mc./sec. for possible four combinations of the signs of  $J_{AX}$  and  $J_{BX}$  with positive  $J_{AB}$ . The observed spectrum (dotted lines) is superposed on each calculated spectrum for comparison.

just the coupling constant,  $J_{AX}$ , calculated from the spectra at the higher resonant frequencies. Thus, it seems reasonable to assume the existence of the long-range coupling between the methyl protons and fluorine in this compound.

In the  $A_3B_2X$  system the relative sign determination of the coupling constants is possible in principle.<sup>5)</sup> Whether it is really possible or not, however, depends upon the relative order of magnitude between the  $J$ 's and  $\delta$ 's. Tentative calculations show that at 15 Mc./sec. the spectrum is sufficiently altered in its appearance by changing the signs of the coupling constants, thus permitting an unambiguous determination of the relative signs for triethylfluorosilane, though not for triethylsilane. It can be assumed that  $J_{AX}$  is positive on the basis of the theoretical considerations by

Karplus<sup>11)</sup> and by McConnell.<sup>12)</sup> Thus, it is sufficient to consider the possible four cases with positive  $J_{AB}$  values. In Fig. 5 the calculated spectra for triethylfluorosilane at 15 Mc./sec. are shown for possible combinations of the signs for  $J_{BX}$  and  $J_{AX}$  using the  $J$ 's and the  $\delta_{AB}$  obtained from the spectra of other resonant frequencies. A close inspection of Figs. 5a—5d suggests that the best fit is obtained when all the signs are alike, i.e., when  $J_{AB}$ ,  $J_{BX}$ , and  $J_{AX}$  are all positive. To make the conclusion more unambiguous, NMR measurements on other similar compounds involving the double resonance experiment will be required. We are now planning to study further along these lines.

11) M. Karplus, *J. Chem. Phys.*, **30**, 11 (1959).

12) H. M. McConnell, *ibid.*, **24**, 460 (1956).

**The Internal Chemical Shift,  $\delta$ .**—The additivity for the  $\delta$  value in the  $\text{Si}(\text{C}_2\text{H}_5)_4\text{—SiCl}_3(\text{C}_2\text{H}_5)$  series was pointed out by Narasimhan and Rogers.<sup>2)</sup> They derived the empirical equation:

$$\delta \text{ for } \text{SiCl}_n(\text{C}_2\text{H}_5)_{4-n} = -0.420 + 0.205n \quad (\text{in p.p.m.})$$

from the observed values for  $\text{Si}(\text{C}_2\text{H}_5)_4$  and its di- and trichloro-derivatives. It is interesting, as they pointed out, to compare the value predicted for triethylchlorosilane from the above equation with the observed value. The predicted value is  $-0.215$  p.p.m., while the observed value obtained in this work is  $-0.22$  p.p.m.; thus, a good agreement is obtained.

The effect of the number of the substituents on the  $\delta$  value in this case can be interpreted on the basis of the inductive mechanism, as has been mentioned by Narasimhan and Rogers.<sup>2)</sup> The increase in the number of the substituents causes the metal atom to withdraw more electrons and results in less shielding on the methylene protons, which in turn leads to a larger  $\delta$  value (including the sign) than that of the compound with fewer substituents.

The result can also be interpreted, however, in terms of the magnetic anisotropy effect. It was pointed out by Spiesecke and Schneider<sup>13)</sup> that the anisotropy contributions to the methyl and the methylene protons in the ethyl halides,  $\text{CH}_3\text{CH}_2\text{X}$ , are in the same direction and of comparable magnitude; thus, on taking the difference (the  $\delta$  value), the effects are largely cancelled. In the present case, the X group is a metal, and in the halides an additional substituent, Y (i.e., a halogen atom), is further attached to the X group. In this instance, the situation is rather different. The  $\alpha$  and the  $\beta$  protons from the metal are now at the  $\beta$ - and the  $\gamma$ -positions respectively in relation to the Y substituent. The  $\gamma$  protons will be little affected by the secondary magnetic field generated by the diamagnetic circulation of electrons at the X-Y bond; therefore, they will suffer no appreciable contribution to shift to a lower field by the Y substituent.<sup>14)</sup> There is no proton at the  $\alpha$ -position relative to the Y substituent. Thus, only the  $\beta$  protons are subjected to a lower field shift, the extent increasing as the number of substituents increases. Thus, the above linear relation only states that the extent of the decrease in the  $\delta$  value is proportional to the number of the Y substituent. The origin of the decrease may be either the inductive or the anisotropy effect, or it may perhaps be both.

On the contrary, the present study clearly

indicates that the effect of the nature of the substituents attached to the metal on the  $\delta$  value results from the magnetic anisotropy of the Y substituent. As may be seen in Table I, there is also a tendency for the  $\delta$  values of the compounds to increase in the descending order of the electronegativity of the Y substituents in the triethylhalogenosilane, as in the case of diethylaluminum monohalides.<sup>3)</sup> On the basis of the inductive mechanism, it would be expected that the  $\delta$  values would become larger when a halogen atom with a larger electronegativity is substituted into the metal, and the order for the  $\delta$  value would be reverse to the above results. Since the magnitude of the magnetic anisotropy effect of halogens increases with an increase in their atomic weight, as has been mentioned earlier, the tendency of the  $\delta$  value can be elucidated on the basis of the anisotropy effect stated above in the triethylhalogenosilanes also.

The authors express their hearty thanks to Mr. Atsuo Tokutake for his assistance in the experimental work.

Government Chemical Industrial  
Research Institute, Tokyo  
Shibuya-ku, Tokyo

## Appendix

The transitions which give the two central lines in question are shown in Table IV, in which such abbreviations for the spin functions as  $A_{I_A, m_A}$ ,  $B_{I_B, m_B} X_{I_X, m_X}$ , are used where  $I_A$  and  $m_A$  are the total spin and  $z$ -component of the angular momentum for the A nuclei respectively. The spin product functions of the states corresponding to these transitions are characterized by containing a  $B_{0,0}$  term. In the  $A_3B_2X$  system,  $\delta_{AX} (= \nu_X - \nu_A)$  is large compared with  $J_{AX}$ , so we have for transition 1:

$$\begin{aligned} & \frac{1}{2} \delta_{AX} + J_{AX} - \frac{1}{2} \sqrt{(\delta_{AX} + J_{AX})^2 + 3J_{AX}^2} \\ &= \frac{1}{2} (\nu_X - \nu_A) + J_{AX} - \frac{1}{2} (\nu_X - \nu_A + J_{AX}) \\ & \times \left\{ 1 + \frac{3}{2} \left( \frac{J_{AX}}{\nu_X - \nu_A + J_{AX}} \right)^2 + \dots \right\} \\ &= \nu_A + \frac{1}{2} J_{AX} \end{aligned}$$

In a similar way, all of the first four transitions in Table IV give the frequency of  $\nu_A + \frac{1}{2} J_{AX}$ , and the other four  $\nu_{AX} - \frac{1}{2} J_{AX}$ . Thus, the transitions

between these energy levels give two intense lines separated by  $J_{AX}$  from each other, the center being at  $\nu_A$ . The relative intensities of the two lines can be shown to be equal. In the  $A_3B_2X$  system, however, the corresponding states, such as  $A_{3/2}, 3/2 B_{0,0}$ ,

13) H. Spiesecke and W. G. Schneider, *ibid.*, **35**, 722 (1961).

14) J. R. Cavanaugh and B. P. Dailey, *ibid.*, **34**, 1099 (1961).

are themselves a stationary state, and all of the transitions between them give a single line at  $\nu_A$ ,

which forms the most intense central line in the  $A_3B_2$  pattern.

TABLE IV. A-TRANSITION CONCERNED WITH  $B_{0,0}$  SPIN STATES

Transition in the limit $J_{AX} \rightarrow 0$		Frequency
1	$A_{3/2,1/2}B_{0,0}X_{1/2,1/2} \rightarrow A_{3/2,3/2}B_{0,0}X_{1/2,1/2}$	$\frac{1}{2} \delta_{AX} + J_{AX} - \frac{1}{2} \sqrt{(\delta_{AX} + J_{AX})^2 + 3J_{AX}^2}$
2	$A_{3/2,-1/2}B_{0,0}X_{1/2,1/2} \rightarrow A_{3/2,1/2}B_{0,0}X_{1/2,1/2}$	$\frac{1}{2} \left( \sqrt{(\delta_{AX} + J_{AX})^2 + 3J_{AX}^2} - \sqrt{\delta_{AX} + 4J_{AX}^2} \right)$
3	$A_{3/2,-3/2}B_{0,0}X_{1/2,1/2} \rightarrow A_{3/2,-1/2}B_{0,0}X_{1/2,1/2}$	$\frac{1}{2} \left( \sqrt{\delta_{AX}^2 + 4J_{AX}^2} - \sqrt{(\delta_{AX} - J_{AX})^2 + 3J_{AX}^2} \right)$
4	$A_{1/2,-1/2}B_{0,0}X_{1/2,1/2} \rightarrow A_{1/2,1/2}B_{0,0}X_{1/2,1/2}$	$\frac{1}{2} \left( \delta_{AX} + J_{AX} - \sqrt{\delta_{AX}^2 - J_{AX}^2} \right)$
5	$A_{3/2,1/2}B_{0,0}X_{1/2,-1/2} \rightarrow A_{3/2,3/2}B_{0,0}X_{1/2,-1/2}$	$\frac{1}{2} \left( -\sqrt{(\delta_{AX} + J_{AX})^2 + 3J_{AX}^2} + \sqrt{\delta_{AX}^2 + 4J_{AX}^2} \right)$
6	$A_{3/2,-1/2}B_{0,0}X_{1/2,-1/2} \rightarrow A_{3/2,1/2}B_{0,0}X_{1/2,-1/2}$	$\frac{1}{2} \left( -\sqrt{\delta_{AX}^2 + 4J_{AX}^2} + \sqrt{(\delta_{AX} - J_{AX})^2 + 3J_{AX}^2} \right)$
7	$A_{2/2,-3/2}B_{0,0}X_{1/2,-1/2} \rightarrow A_{3/2,-1/2}B_{0,0}X_{1/2,-1/2}$	$\frac{1}{2} \delta_{AX} - J_{AX} - \frac{1}{2} \sqrt{(\delta_{AX} - J_{AX})^2 + 3J_{AX}^2}$
8	$A_{1/2,-1/2}B_{0,0}X_{1/2,-1/2} \rightarrow A_{1/2,1/2}B_{0,0}X_{1/2,-1/2}$	$\frac{1}{2} \left( \delta_{AX} - J_{AX} - \sqrt{\delta_{AX}^2 - J_{AX}^2} \right)$